

# Enhancing Visual Feature Attribution via Weighted Integrated Gradients

Tran Duc Tuan Kien<sup>a</sup>, Nguyen Trong Tam<sup>a</sup>, Nguyen Hoang Son<sup>a</sup>, Khoat Than<sup>a</sup>, Nguyen Duc Anh<sup>a,\*</sup>

<sup>a</sup>Hanoi University of Science and Technology, No 1 Dai Co Viet, Hanoi, 100000, Hanoi, Vietnam

---

## Abstract

Integrated Gradients (IG) is a widely used attribution method in explainable AI, particularly in computer vision applications where reliable feature attribution is essential. A key limitation of IG is its sensitivity to the choice of baseline (reference) images. Multi-baseline extensions such as Expected Gradients (EG) assume uniform weighting over baselines, implicitly treating baseline images as equally informative. In high-dimensional vision models, this assumption often leads to noisy or unstable explanations. This paper proposes Weighted Integrated Gradients (WG), a principled approach that evaluates and weights baselines to enhance attribution reliability. WG introduces an unsupervised criterion for baseline suitability, enabling adaptive selection and weighting of baselines on a per-input basis. The method not only preserves core axiomatic properties of IG but also providing improved theoretical guarantees on quality of explanation over EG. Experiments on commonly used image datasets and models show that WG consistently outperforms EG, yielding 1035% improvements in attribution fidelity. WG further identifies informative baseline subsets, reducing unnecessary variability while maintaining high attribution accuracy. By moving beyond the idea that all baselines matter equally, Weighted Integrated Gradients offers a clearer and more reliable way to explain computer-vision models, improving both understanding and practical usability in explainable AI.

**Keywords:** Explainable AI, Feature Attribution, Expected Gradients, Computer Vision

---

## 1. Introduction

Explainable AI (XAI) is increasingly important as deep neural networks, especially computer vision tasks such as classification, detection, and segmentation. In these applications, understanding model behavior is essential for trust, safety, and diagnostics [1, 2]. A central direction in XAI is feature attribution, which quantifies how individual pixels or regions contribute to a model's output. Among attribution methods, Integrated Gradients (IG) [3] is a key technique, built on path-based attribution and related to Shapley values [4]. IG integrates gradients along a straight-line path from a baseline to the input to derive feature importance.

While IG satisfies several desirable axioms, it faces practical challenges. Prior work highlights three issues for path-based methods: baseline choice, path construction, and counterintuitive attributions [5]. Of these, baseline selection is the most critical in vision, where no universally "neutral" reference image exists. Common baselines such as black, white, blurred, or random images often yield inconsistent explanations, and the theoretical link between baseline choice and attribution behavior remains poorly understood [6].

To mitigate sensitivity to baselines, the Expected Gradients (EG) method [7] averages IG attributions across many baselines, showing its advantage over other methods such as Grad-CAM [8]. Although EG improves robustness, it assumes all baselines are equally informative. In high-dimensional vision models, however, baselines vary greatly in their relevance.

When many are low quality, uniform averaging can distort explanations by allowing poor baselines to dominate or dilute the final attribution.

We propose a new approach that assesses the *fitness* of each baseline and uses it to form a principled weighted aggregation. Our key insight is that baseline quality depends jointly on both the input and the baseline; hence each baseline should contribute proportionally to its explanatory relevance. Unlike EG, our method assigns *data-driven weights* that emphasize baselines producing more faithful explanations.

We define an unsupervised fitness function that evaluates baseline suitability solely from model behavior, requiring no annotation or domain knowledge. An efficient algorithm computes this fitness in  $O(\log n)$ , enabling scalability to large baseline sets. These scores are normalized into weights used to aggregate IG attributions. Experiments on standard vision benchmarks show that this weighted strategy improves attribution accuracy, fidelity, and stability over existing multi-baseline methods.

Beyond improved interpretability, the framework naturally supports filtering low-quality baselines, reducing computation while maintaining reliable attributions. This dual benefit makes the method well suited for modern vision models requiring fast yet robust explanation tools. Experiments show that WG boosts attribution quality by 24.8% on average across diverse models. WG preserves IGs theoretical foundations while adding an efficient, adaptive, data-driven weighting mechanism, resulting in a scalable and accurate attribution method for deep learning systems.

In summary, we address key challenges in IG-based attribu-

---

\*Corresponding author. Email: anhnd@soict.hust.edu.vn. The paper is under consideration at Pattern Recognition Letters.

tion by introducing a principled, adaptive mechanism for evaluating and weighting baselines, improving stability and interpretability while preserving core axiomatic properties of path-based methods.

## 2. Related work

Explainable AI (XAI) methods are often grouped into perturbation-based, backpropagation-based, and attention-based approaches. Perturbation methods estimate feature importance by masking or altering inputs but are computationally expensive for high-resolution models [9]. Backpropagation-based techniques propagate relevance using gradients or attribution rules and offer a far more efficient alternative [10]. Attention-based methods highlight influential tokens via transformer attention, though their interpretability remains debated [11]. Among these, gradient-based backpropagation strikes the best balance between efficiency and interpretability and forms the foundation of our approach.

*Integrated Gradients* (IG) [3] attributes importance by integrating gradients from a baseline to the input, but its effectiveness depends heavily on the chosen baseline [5], which is particularly problematic in vision tasks lacking a neutral reference image. To address this, prior work has explored improved baseline strategies and multi-baseline formulations, such as learned or sampled baselines [7], as well as path-based refinements that better align with perceptual structure [12]. While some methods introduce weighting schemes for attribution, none explicitly focus on weighting IG baselines.

We fill this gap with *Weighted Integrated Gradients* (WG), a framework that assigns input-dependent baseline weights using an unsupervised fitness measure. Unlike EGs uniform averaging or SIGs sampling-based proportionality, WG selectively emphasizes baselines that yield faithful local explanations, improving reliability and stability.

## 3. Background

In this section, we briefly review the key concepts of Integrated Gradients and Expected Gradients, and then highlight the limitations of the latter. Reformulating Integrated Gradients as a gradient path integral and Expected Gradients as a uniform expectation over baselines reveals a central drawback of EG: its assumption that all baselines contribute equally, regardless of their relevance to a specific input. This oversimplified weighting scheme leads to suboptimal and unstable attributions. These limitations motivate our proposed method, which introduces refined, input-aware baseline weighting for more accurate and reliable explanations.

### 3.1. Intergrated Gradient

Integrated Gradients (IG) [3] computes feature attributions by accumulating gradients along a path from a baseline  $x'$  to the input  $x$ . Inspired by game-theoretic foundations, IG begins at a reference point, ideally a neutral state carrying minimal information, and traces a continuous trajectory toward  $x$ , capturing how features contribute to the model’s prediction.

Formally, for a classifier, a class  $c$ , and an input  $x$ , let  $f_c(x)$  denote the model’s score for class  $c$ . The attribution for the  $i$ th feature is defined as:

$$\text{IG}_i(x, x') := (x_i - x'_i) \times \int_0^1 \frac{\partial f(x' + \alpha(x - x'))}{\partial x_i} d\alpha, \quad (1)$$

where  $\frac{\partial f(x)}{\partial x_i}$  is the gradient of  $f$  along the  $i$ th feature and  $\alpha$  parameterizes the interpolated coefficient of points that lie between input and the reference point  $x'$  ( $\alpha \in [0, 1]$ ). This integral captures each features contribution by averaging its gradients influence across the path.

Empirical evidence underscores that baseline choice profoundly impacts explanation quality, yet no rigorous theory defines an optimal  $x'$  for arbitrary inputs. A baseline effective for one image may falter for another, necessitating laborious, image-specific tuning that remains suboptimal and impractical. This variability exposes a gap in path-based XAI: the lack of a principled, adaptive strategy for baseline selection.

### 3.2. Expected Gradient

To address the baseline selection issue in Integrated Gradients (IG), Expected Gradients (EG) [7] introduces a widely used solution that averages IG over multiple baselines instead of relying on a single one. By uniformly sampling baselines from a pre-selected set  $D' = \{x^{(k)}\}_{k=1}^n$ , EG approximates the expected attribution:

$$\text{EG}_i(x) = \int_{x'} \text{IG}_i(x, x') p_D(x') dx' \approx \frac{1}{n} \sum_{k=1}^n \text{IG}_i(x, x^{(k)}), \quad (2)$$

This approach captures diverse perspectives from multiple reference points, producing more stable explanations. However, EG assigns uniform weights to all baselines, treating them as equally informative even though some align well with decision boundaries while others introduce noise. As a result, uniform averaging can dilute useful signals and distort the models rationale.

To address this, we propose Weighted Integrated Gradients (WG), which assigns input-specific weights based on each baselines ability to yield accurate, informative gradients. By emphasizing high-fitness baselines, WG produces more precise and interpretable attributions, improving the fidelity of gradient-based explanations.

## 4. Proposed Method

In this section, we propose Weighted Integrated Gradients (WG), a novel advancement that redefines baseline selection in Integrated Gradients (IG) through a perturbation-based fitness measure. WG departs from the limitations of prior methods by assigning weights to baselines according to their explanatory fidelity, thereby enhancing the precision and robustness of feature attributions.

Consider a differentiable model  $f : \mathbb{R}^d \rightarrow \mathbb{R}$ , an input  $x \in \mathbb{R}^d$ , and a set of baselines  $D' = \{x^{(k)}\}_{k=1}^n$ . The WG attribution for feature ( $i$ ) is defined as:

$$\begin{aligned} \text{WG}_i(x) &= \sum_{k=1}^n w_k \cdot \text{IG}_i(x, x^{(k)}), \\ &= \sum_{k=1}^n w_k (x_i - x_i^{(k)}) \int_0^1 \frac{\partial f(x^{(k)} + \alpha(x - x^{(k)}))}{\partial x_i} d\alpha \end{aligned} \quad (4)$$

where  $w_k$  represents the weight of the ( $k$ )-th baseline  $x^{(k)}$ , derived from its fitness, and the integral computes the IG attribution for each baseline. By modulating the influence of each baseline via  $w_k$ , WG ensures that more informative reference points dominate the aggregation, yielding a final explanation that better reflects the models decision-making process. In the following, we describe a strategy for calculating  $w_k$ .

#### 4.1. Fitness Measure Based on Perturbation

Perturbation offers a natural and intuitive method for evaluating individual elements in complex systems. In explainable AI, particularly for baseline selection in Integrated Gradients (IG), it helps assess each baselines impact by modifying or removing input features and observing the resulting output changes.

This method eliminates the need for manual annotations, relying on the model itself to assess output variations, making it efficient and objective. To quantify the quality of a baseline for a given input, we propose a fitness function  $D_\alpha$ , defined as the minimum number of features that must be masked to reduce the model’s output to  $\alpha\%$  of its original score:

$$D_\alpha = \min \{|S| : S \subseteq F, f(x \circ M(S)) \leq \alpha \cdot f(x)\} \quad (5)$$

where  $M(S)$  masks features in  $S$ , and  $x \circ M(S)$  denotes the masked input. A smaller  $D_\alpha$  implies the baseline effectively highlights influential features, since fewer need to be masked to impact the output significantly.

In Weighted Integrated Gradients (WG), we assign weights based on this fitness:

$$w_k \propto \frac{1}{D_\alpha} \quad (6)$$

ensuring that baselines with higher explanatory power (lower  $D_\alpha$ ) contribute more to the final attribution. This approach is both principled and unsupervised, aligning attribution fidelity with model sensitivity.

To compute  $D_\alpha$ , the minimal number of features to mask to reduce the models output score to  $\alpha\%$  of its original value, a naive exhaustive search would incur a prohibitive  $O(n)$  time complexity, where  $n$  is the number of features. Leveraging the monotonicity of score reduction upon feature removal, we propose Algorithm 1, an efficient binary search strategy, achieving a time complexity of  $O(\log n)$  per baseline. The algorithm iteratively adjusts the proportion of features masked guided by their importance scores (e.g., IG attributions) until the target score is approximated within a tolerance  $\epsilon$ .

#### 4.2. Algorithm for Efficient Fitness Calculation

---

##### Algorithm 1 Compute\_D\_alpha

---

**Require:**  $x$ : input data (e.g., image)  
**Require:**  $attr$ : feature importance scores (e.g., IG attributions)  
**Require:**  $f$ : model function (classifier)  
**Require:**  $\alpha$ : target score reduction ratio ( $0 < \alpha < 1$ )  
**Require:**  $neutral$ : neutral value for masked features  
**Require:**  $\epsilon$ : convergence threshold  
**Ensure:**  $d_\alpha$ : minimal number of removal pixels

- 0:  $target\_score \leftarrow \alpha \cdot f(x)$
- 1:  $low \leftarrow 0$
- 2:  $high \leftarrow \text{count}(x)$
- 3: **while**  $low \leq high$  **do**
- 4:    $mid \leftarrow \lfloor (low + high)/2 \rfloor$
- 5:    $mask \leftarrow \text{FindMask}(attr, mid)$
- 6:    $x' \leftarrow x \cdot (1 - mask) + neutral \cdot mask$
- 7:   **if**  $|f(x') - target\_score| < \epsilon$  **then**
- 8:     **return**  $mid$
- 9:   **else if**  $f(x') < target\_score$  **then**
- 10:      $low \leftarrow mid + 1$
- 11:   **else**
- 12:      $high \leftarrow mid - 1$
- 13:   **end if**
- 14: **end while**
- 15: **return**  $mid$

---

## 5. Theoretical Analysis

Since WG is defined as a non-negative weighted sum of Integrated Gradients (IG) across multiple baselines, and IG satisfies *Implementation Invariance* and *Effectiveness* [3], WG naturally inherits these two properties. Regarding completeness, IG satisfies the standard axiom with respect to a *single* baseline, whereas WG satisfies an analogous *generalized completeness* property: the total WG attribution equals the model output at  $x$  minus the *weighted expected baseline output*.

Beyond these axiomatic considerations, we further study WG from a probabilistic viewpoint. Each IG attribution vector is interpreted as a probability distribution over features, and we assume that baselines with better fitness scores  $D_\alpha$  tend to place more probability mass on truly relevant features. Under this mild assumption, we show that WG increases the expected relevance of sampled baselines and provides tighter finite-sample probabilistic guarantees than equal-weight averaging (EG). For detailed statements and proofs, please refer to Appendix A.

### 5.1. Probabilistic model

For each baseline  $x^{(k)}$ , we define the normalized positive IG profile as

$$p_j^{(k)} = \frac{[IG_j(x, x^{(k)})]_+}{\sum_{\ell=1}^d [IG_\ell(x, x^{(k)})]_+}, \quad j = 1, \dots, d, \quad (7)$$

where  $[a]_+ := \max(a, 0)$  denotes the positive part. By construction,

$$\sum_{j=1}^d p_j^{(k)} = 1.$$

Interpret  $p^{(k)}$  as a probability distribution on feature indices. Let  $R(x) \subseteq \{1, \dots, q\}$  be the (unknown) set of truly relevant features. Define the relevance quality

$$Q_k(x) = \sum_{j \in R(x)} p_j^{(k)} = \Pr_{J \sim p^{(k)}}(J \in R(x)).$$

Let  $u_k = 1/n$  be the EG weights and

$$w_k = \frac{D_\alpha(x^{(k)})^{-1}}{\sum_{j=1}^n D_\alpha(x^{(j)})^{-1}}$$

be the WG weights derived from the fitness scores  $D_\alpha(x^{(k)})$ .

**Assumption 1** (Fitness–relevance monotonicity). *Order baselines so that*

$$D_\alpha(x^{(1)}) \leq D_\alpha(x^{(2)}) \leq \dots \leq D_\alpha(x^{(n)}).$$

Assume that better fitness implies higher relevance:

$$D_\alpha(x^{(k)}) \leq D_\alpha(x^{(k')}) \Rightarrow Q_k(x) \geq Q_{k'}(x).$$

### 5.2. WG improves expected relevance

**Proposition 1** (WG favors relevant baselines more than EG). *Under Assumption 1,*

$$\mathbb{E}_{K \sim \text{WG}}[Q_K(x)] = \sum_{k=1}^n w_k Q_k(x) \geq \sum_{k=1}^n u_k Q_k(x) = \mathbb{E}_{K \sim \text{EG}}[Q_K(x)],$$

with strict inequality unless all  $Q_k(x)$  are equal.

Thus, sampling a baseline according to WG is more likely to yield one that places higher mass on truly relevant features, compared to EG.

### 5.3. Finite-sample advantage of WG

Let the aggregated WG attribution have normalized profile  $p^{\text{WG}}$ , and define its relevance probability as

$$p_{\text{WG}}(x) = \sum_{j \in R(x)} p_j^{\text{WG}} = \Pr_{J \sim p^{\text{WG}}}(J \in R(x)).$$

Define  $q_{\text{EG}}(x)$  analogously from  $p^{\text{EG}}$ . Sampling  $m$  features independently from  $p^{\text{M}}$  for  $\text{M} \in \{\text{WG}, \text{EG}\}$  yields the empirical relevance fraction

$$\hat{q}_{\text{M}}(x, m) = \frac{1}{m} \sum_{t=1}^m \mathbf{1}\{J_t^{\text{M}} \in R(x)\}.$$

**Theorem 2** (High-probability relevance guarantee for WG). *Let  $\Delta(x) := q_{\text{WG}}(x) - q_{\text{EG}}(x) \geq 0$ . For any  $m \geq 1$  and any  $\delta \in (0, 1)$ ,*

$$\Pr(\hat{q}_{\text{WG}}(x, m) \leq q_{\text{EG}}(x)) \leq \exp(-2m \Delta(x)^2).$$

Equivalently, to guarantee

$$\Pr(\hat{q}_{\text{WG}}(x, m) > q_{\text{EG}}(x)) \geq 1 - \delta,$$

it suffices to choose

$$m \geq \frac{1}{2 \Delta(x)^2} \log\left(\frac{1}{\delta}\right).$$

Theorem 2 shows that WG achieves a strictly larger relevance margin  $\Delta(x)$  than EG (by Proposition 1), and this margin translates directly into an exponential finite-sample advantage. With a small sampling budget  $m$ , WG is substantially more likely than EG to allocate probability mass to truly relevant features.

Under this simple probabilistic relevance model, WG improves both the *expected* relevance of sampled baselines and the *finite-sample* relevance probability of the aggregated attribution. In contrast, EG treats all baselines equally and therefore cannot exploit variation in baseline quality, whereas WG systematically amplifies high-fitness, high-relevance baselines.

## 6. Experiments

In this section, we present a comprehensive evaluation of our proposed Weighted Integrated Gradients method, benchmarking it against established techniques in explainable AI. Building upon the foundational Integrated Gradients framework, WG introduces a novel fitness-weighted baseline aggregation strategy to address the critical challenge of baseline selection, thereby enhancing the accuracy and stability of feature attributions. Our experiments are designed to showcase WGs robustness across diverse models and datasets, demonstrating its superiority in delivering precise and interpretable explanations for complex deep learning systems, and confirming the advantages in the theoretical analysis <sup>1</sup>.

### 6.1. Experimental Setup

#### Baseline:

We evaluate Weighted Integrated Gradients (WG) against prominent XAI methods, with a primary focus on Expected Gradients (EG) [7], which already showed the advantage over existing explanation method [8]. WG enhances this by weighting baselines via a fitness score and optionally filtering low-quality references to improve efficiency and attribution fidelity. For each input, we sample 5-10 baselines, aligning with EGs setup but applying our weighted aggregation to better capture meaningful feature contributions.

#### Models and Datasets:

Experiments are conducted using pretrained PyTorch models across diverse architectures: DenseNet121, ResNet50, ResNet101, VGG16, and VGG19. We evaluate on ImageNet and COCO, following prior works [3, 13]. To ensure interpretability-focused analysis, we select samples where the

<sup>1</sup>The implementation is available at: [https://github.com/tamnt240904/weighted\\_ig](https://github.com/tamnt240904/weighted_ig)

model prediction is correct, enabling a fair comparison of explanation quality across methods.

### Evaluation metrics: AUC of Deletion

The AUC of Deletion measures explanation quality by evaluating how rapidly a model’s confidence drops when important features (ranked by an attribution method  $\phi(x)$ ) are progressively removed. For an input  $x$  and class  $c$ , a perturbed version of the input  $x$  is created by masking the top- $p\%$  features in  $\phi(x)$  by a mask  $M_p(\phi(x))$ , and the model’s retained confidence is:

$$\text{Deletion Score}(x, \phi(x), p) = f_c(x \circ M_p(\phi(x)))$$

The AUC of Deletion is defined by aggregating scores over all perturbation levels ( $p = 0\%$  to  $100\%$ ):

$$\begin{aligned} \text{AUC of Deletion} &= \int_0^1 \text{Deletion Score}(x, \phi(x), p) dp \\ &\approx \frac{1}{N} \sum_{i=1}^N f_c(x \circ M_{p_i}(\phi(x))), \quad p_i = \frac{i}{N} \end{aligned}$$

A lower AUC indicates better explanations, as important features cause sharper confidence drops when removed. This metric is threshold-free, robust to noise, and aligns with the principle that ideal attributions should most disrupt the prediction when key features are removed. It serves as a core evaluation tool in our analysis of WGs’ effectiveness.

### AUC of Overlap

While AUC of Deletion measures the effect of removing important features, it does not assess whether attributions align with human-recognizable regions. To address this, we introduce the *AUC of Overlap*, a supervised metric evaluating how well attribution maps match ground-truth segments.

Given a segmentation mask  $S$  of size  $|S|$ , let  $T_p$  be the top  $p|S|$  pixels of  $\phi(x)$ . The overlap at proportion  $p$  is:

$$\text{Overlap}(p) = \frac{|T_p \cap S|}{p|S|}.$$

The metric aggregates overlap across  $p \in (0, 1]$ :

$$\text{AUC of Overlap} = \int_0^1 \text{Overlap}(p) dp \approx \frac{1}{N} \sum_{i=1}^N \text{Overlap}\left(\frac{i}{N}\right).$$

A higher AUC indicates stronger spatial alignment between the explanation and the ground-truth object, making this metric essential for evaluating interpretability in vision tasks.

**Fitness Function:** To compute the fitness measure  $D_\alpha$ , we set the parameter  $\alpha = 0.5$ , corresponding to a 50% reduction in model confidence—a threshold with deep scientific relevance. In fields like toxicology, the 50% threshold (e.g., LC50 or LD50) is a standard benchmark for assessing median effects, reflecting a critical inflection point. In explainable AI,  $\alpha = 0.5$  identifies the feature set whose removal halves the model’s score, capturing a pivotal transition where confidence fluctuates significantly, just beyond the model’s initial robustness and before saturation effects dominate in gradient-based methods. This

choice ensures that  $D_\alpha$  targets a meaningful and interpretable point of model behavior.

**Optimization:** For computational efficiency, we employ an above binary search algorithm to compute  $D_\alpha$ , achieving a time complexity of  $O(\log n)$ , where  $n$  is the number of features. We set a convergence threshold of  $\epsilon = 0.01$  and limit the number of iterations to 100, ensuring both precision and scalability. These optimization strategies enable WG to deliver reliable and interpretable results while maintaining computational tractability, making it well-suited for large-scale applications.

## 6.2. Qualitative Analysis

### a. Evaluating on AUC of Deletion and Overlap score

Table 1 compares Expected Gradients (EG) and our proposed Weighted Integrated Gradients (WG) across six backbone models using two metrics: AUC of Deletion (lower is better) and AUC of Overlap (higher is better). Reported values include mean  $\pm$  standard deviations, relative improvements, and  $p$ -values from significance t-tests.

WG significantly outperforms EG on Deletion AUC for all models. For instance, on DenseNet121, WG reduces the AUC from 0.082 to 0.062 (24.40% improvement,  $p = 0.000$ ). Similar improvements are observed on MobileNetV2 (26.21%,  $p = 0.007$ ), ResNet50 (35.28%,  $p = 0.002$ ), ResNet101 (34.40%,  $p = 0.001$ ), VGG16 (24.15%,  $p = 0.002$ ), and VGG19 (24.65%,  $p = 0.020$ ), indicating WGs superior ability to identify impactful features.

WG also consistently improves Overlap AUC, achieving better alignment with salient regions. Notable gains include 17.20% on ResNet101, 14.72% on ResNet50, 15.03% on VGG16, and 15.34% on VGG19, with over 10% improvement even on MobileNetV2 and DenseNet121—all statistically significant.

A deeper analysis confirms WGs robustness: on shallow architectures like VGG16/19, it brings modest gains in Overlap AUC but significant improvements in Deletion AUC, reflecting better feature selection. On deeper models such as DenseNet121 and ResNet101, WG achieves larger gains on both metrics, demonstrating its scalability and effectiveness in modeling complex feature hierarchies. For visualization, Fig. 2 illustrates that our method, Weighted Integrated Gradients (WG), produces sharper and more relevant saliency maps compared to the baseline Expected Gradients across various models.

These results support our core hypothesis: weighting baselines by fitness mitigates EGs’ uniform sampling bias, yielding more accurate and interpretable attributions. WG achieves an average 24.8% improvement in Deletion AUC and consistent gains in Overlap AUC. Its ability to discard suboptimal baselines (see Section 3) also improves efficiency without compromising accuracy. Together, these findings affirm WGs’ practical and theoretical strengths for reliable explanations in real-world applications.

Table 1: Comparison of Expected Gradients and Weighted Integrated Gradients performance across Models. For AUC of Deletion, smaller is better, for AUC of Overlap, higher is better.

Metrics	Model	EG	WG (Ours)	Rel. I (%)	p-value
Mean AUC of Deletion ( $\downarrow$ )	DenseNet121	0.082 $\pm$ 0.094	<b>0.062 <math>\pm</math> 0.088</b>	24.40	0.000
	MobileNetV2	0.021 $\pm$ 0.033	<b>0.015 <math>\pm</math> 0.024</b>	26.21	0.007
	ResNet50	0.045 $\pm$ 0.068	<b>0.029 <math>\pm</math> 0.048</b>	35.28	0.002
	ResNet101	0.057 $\pm$ 0.081	<b>0.037 <math>\pm</math> 0.071</b>	34.40	0.001
	VGG16	0.035 $\pm$ 0.058	<b>0.026 <math>\pm</math> 0.052</b>	24.15	0.002
	VGG19	0.029 $\pm$ 0.047	<b>0.022 <math>\pm</math> 0.037</b>	24.65	0.020
Mean AUC of Overlap ( $\uparrow$ )	DenseNet121	0.418 $\pm$ 0.172	<b>0.461 <math>\pm</math> 0.171</b>	10.03	0.010
	MobileNetV2	0.418 $\pm$ 0.191	<b>0.461 <math>\pm</math> 0.179</b>	11.34	0.001
	ResNet50	0.390 $\pm$ 0.187	<b>0.447 <math>\pm</math> 0.186</b>	14.72	0.001
	ResNet101	0.391 $\pm$ 0.185	<b>0.458 <math>\pm</math> 0.180</b>	17.20	0.001
	VGG16	0.423 $\pm$ 0.178	<b>0.488 <math>\pm</math> 0.177</b>	15.03	0.000
	VGG19	0.427 $\pm$ 0.179	<b>0.457 <math>\pm</math> 0.180</b>	15.34	0.035

Table 2: Comparison of WG and Filter-WG. For deletion, smaller is better; for overlap, higher is better.

Metrics	Model	WG (Ours)	Filtered-WG (Ours)
Mean AUC of Deletion ( $\downarrow$ )	DenseNet121	0.06198	<b>0.06160</b>
	MobileNetV2	0.01519	<b>0.01497</b>
	ResNet50	0.02879	<b>0.02870</b>
	ResNet101	0.03726	<b>0.03648</b>
	VGG16	0.02686	<b>0.02679</b>
	VGG19	0.02204	<b>0.02199</b>
Mean AUC of Overlap ( $\uparrow$ )	DenseNet121	0.4617	<b>0.46210</b>
	MobileNetV2	<b>0.4613</b>	0.4606
	ResNet50	0.4472	<b>0.4469</b>
	ResNet101	0.4579	<b>0.4591</b>
	VGG16	0.4882	<b>0.4897</b>
	VGG19	<b>0.4571</b>	0.4569

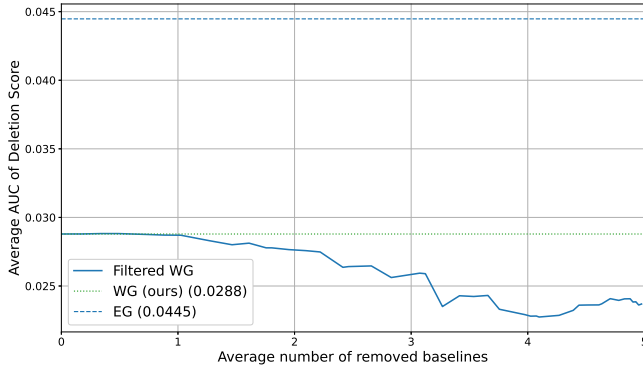


Figure 1: The average AUC of Deletion Score for Filtered WG using ResNet50 architecture. Low-quality baselines were removed based on their fitness scores, resulting in more trustworthy final explanations, as reflected by a reduction in the AUC of the Deletion Score. The fitness score serves as an effective criterion to balance the trade-off between computational efficiency and explanation faithfulness

### b. Effective baselines selection mechanism

To address the computational overhead of multi-baseline attribution methods while preserving explanation accuracy, we propose an effective baseline selection mechanism for WG. After

computing the fitness value  $D_\alpha$  for each baseline, we filter out those with low fitness scores (high  $D_\alpha$ ), aggregating only high-fitness baselines. This strategy minimizes the impact of poor baselines, reduces the computational cost of processing them, and ensures that the explanation is driven by the most informative baselines, enhancing both efficiency and attribution quality.

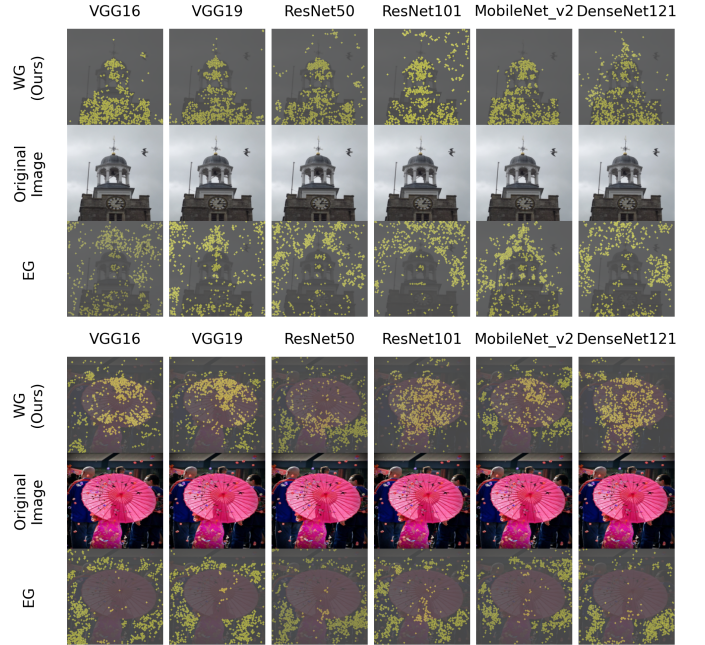


Figure 2: Saliency map comparisons across different models (columns) and methods (rows). The top row is our proposed method, while the bottom row employs Expected Gradients. Our proposed method, Weighted Integrated Gradients (WG), consistently outperforms the baseline approach by focusing more sharply on the main object, demonstrating superior precision and relevance in feature attribution across all models.

We then compare the performance between WG (original version with all baselines with fitness weights), and Filtered WG (WG with low-fitness baselines removed). Table 2 reports the results on ImageNet across various models.

Table 2 compares WG and its Filtered-WG variant using Mean AUC of Deletion (lower is better) and Mean AUC of Overlap (higher is better), assessing attribution robustness and faithfulness.

Filtered-WG consistently maintains or improves WGs performance. For Deletion AUC, it yields lower scores on DenseNet121 (0.06198 0.06160), MobileNetV2 (0.01519 0.01497), and ResNet101 (0.03726 0.03648), indicating more precise attributions. For Overlap AUC, it slightly improves scores on ResNet101 and VGG16, with minimal decline on MobileNetV2.

Overall, Filtered-WG enhances attribution quality by removing low-fitness baselines, improving both interpretability and efficiency without sacrificing performance.

We further analyze the effect of removing low-fitness baselines incrementally, comparing WG with Expected Gradients. Figure 1 plots the average AUC of Deletion Score as we remove 1 to 5 low-fitness baselines.

Figure 1 shows that WGs AUC remains stable, dropping from 0.02879 to a minimum of 0.0140 after removing 4 low-fitness baselines, then slightly rising to 0.015 after 5 removals. This consistent gap (0.013-0.015) highlights WGs robustness: filtering weaker baselines preserves or improves performance while reducing computational cost.

Performance peaks at 4 removals, suggesting an optimal balance. Beyond that, further filtering degrades performance, confirming that some diversity among baselines is beneficial.

These results align with WGs variance-reduction principle (Section 5.4), as filtering noisy baselines yields sharper attributions. Practically, this reduces computation by 40-50% while sustaining or improving attribution quality, enhancing WGs suitability for real-world XAI in complex, resource-constrained settings.

## 7. Conclusion

In this study, we introduced Weighted Integrated Gradients (WG) for Feature Attribution. Unlike previous approaches that treat all baselines equally, WG autonomously evaluates the relevance of each baseline and assigns appropriate weights. WG meets essential requirements for a feature attribution method, including completeness, sensitivity, and implementation invariance, while also offering greater stability with lower variance. Experimental results on key metrics, such as AUC of Deletion and Overlap, demonstrated the superiority of WG over existing methods. Additionally, WGs weighting mechanism facilitates better baseline selection and filtering, maintaining performance while reducing computational costs.

## Acknowledgement

This research is funded by Hanoi University of Science and Technology (HUST) under project number T2024-PC-040.

## Declaration of generative AI and AI-assisted technologies in the manuscript preparation process.

During the preparation of this work the author(s) used ChatGPT in order to copyedit and text refinement. After using this tool/service, the author(s) reviewed and edited the content as needed and take(s) full responsibility for the content of the published article.

## Appendix A. Proof Sketches

*Proof sketch of Proposition 1.* Under Assumption 1, the sequence  $(Q_k(x))$  is nonincreasing in  $k$ . The WG weights  $(w_k)$  form a nonincreasing sequence (since  $w_k \propto 1/D_\alpha(x^{(k)})$ ), while EG uses uniform weights. Rearrangement inequality or Abel summation on two weight vectors and a sorted sequence yields  $\sum_k w_k Q_k \geq \sum_k u_k Q_k$ , with strict inequality unless all  $Q_k$  are identical.  $\square$

*Proof sketch of Theorem 2.* Let  $X_t^{\text{WG}} = \mathbf{1}\{J_t^{\text{WG}} \in R(x)\}$ . Then  $\hat{q}_{\text{WG}} = \frac{1}{m} \sum_{t=1}^m X_t^{\text{WG}}$ , with  $\mathbb{E}[X_t^{\text{WG}}] = q_{\text{WG}}(x)$  and  $X_t^{\text{WG}} \in [0, 1]$ . Hoeffding’s inequality gives

$$\Pr(\hat{q}_{\text{WG}} \leq q_{\text{WG}} - \varepsilon) \leq \exp(-2m\varepsilon^2).$$

Setting  $\varepsilon = \Delta(x)$  and using  $q_{\text{EG}} = q_{\text{WG}} - \Delta(x)$  yields the stated bound.  $\square$

## References

- [1] R. Dwivedi, P. Kothari, D. Chopra, M. Singh, R. Kumar, An efficient ensemble explainable ai (xai) approach for morphed face detection, Pattern Recognition Letters 184 (2024) 197–204.
- [2] N. Koenen, M. N. Wright, Toward understanding the disagreement problem in neural network feature attribution, in: World Conference on Explainable Artificial Intelligence, Springer, 2024, pp. 247–269.
- [3] M. Sundararajan, A. Taly, Q. Yan, Axiomatic attribution for deep networks, in: International conference on machine learning, PMLR, 2017, pp. 3319–3328.
- [4] M. Sundararajan, A. Najmi, The many shapley values for model explanation, in: International conference on machine learning, PMLR, 2020, pp. 9269–9278.
- [5] N. Akhtar, M. A. Jalwana, Towards credible visual model interpretation with path attribution, in: International Conference on Machine Learning, PMLR, 2023, pp. 439–457.
- [6] P. Sturmfels, S. Lundberg, S.-I. Lee, Visualizing the impact of feature attribution baselines, Distill 5 (1) (2020) e22.
- [7] G. Erion, J. D. Janizek, P. Sturmfels, S. M. Lundberg, S.-I. Lee, Improving performance of deep learning models with axiomatic attribution priors and expected gradients, Nature machine intelligence 3 (7) (2021) 620–631.
- [8] L. Klein, C. Lüth, U. Schlegel, T. Bungert, M. El-Assady, P. Jäger, Navigating the maze of explainable ai: A systematic approach to evaluating methods and metrics, Advances in Neural Information Processing Systems 37 (2024) 67106–67146.
- [9] J. Li, W. Monroe, D. Jurafsky, Understanding neural networks through representation erasure, arXiv preprint arXiv:1612.08220 (2016).
- [10] J. T. Springenberg, A. Dosovitskiy, T. Brox, M. Riedmiller, Striving for simplicity: The all convolutional net, arXiv preprint arXiv:1412.6806 (2014).
- [11] J. Vig, Bertviz: A tool for visualizing multihead self-attention in the bert model, in: ICLR workshop: Debugging machine learning models, Vol. 3, 2019.

- [12] S. Xu, S. Venugopalan, M. Sundararajan, Attribution in scale and space, in: Proceedings of the IEEE/CVF Conference on Computer Vision and Pattern Recognition, 2020, pp. 9680–9689.
- [13] R. Yang, B. Wang, M. Bilgic, Idgi: A framework to eliminate explanation noise from integrated gradients, in: Proceedings of the IEEE/CVF Conference on Computer Vision and Pattern Recognition, 2023, pp. 23725–23734.